Overcoming Gassmann's equation limitations in reservoir rocks

Fabien Allo[1] and Lev Vernik[2]

Abstract

Velocities of low-frequency seismic waves and, in most rocks, sonic logging waves depend on the compressibility of the undrained rock, which is conventionally computed from the drained rock compressibility using Gassmann's equation. Although more comprehensive and accurate alternatives exist, the simplicity of the equation has made it the preferred fluid substitution model for geoscience applications. In line with recent publications, we show that Gassmann's equation strictly applies only to rocks with a microhomogeneous void space microstructure that is devoid of cracks and microcracks. We use a rock physics model that separates the respective compliance contributions of pores and cracks on dry (drained) moduli and show that Gassmann's model does not apply to rocks with measurable crack density. A fourth independent bulk modulus (in addition to the bulk moduli of the mineral matrix, dry frame, and saturating fluid) is required to take the effect of cracks into account and perform fluid substitution modeling for rocks with pores and cracks more accurately than prescribed by Gassmann's equation. Therefore, we propose combining the Vernik-Kachanov model with Brown-Korringa's equation for more reliable modeling of undrained bulk compressibility for reservoir rocks with measurable crack density. To conclude, a practical quantification of the applicability of Gassmann's equation based on the combined effects of crack density and stress sensitivity is proposed.

Undrained compressibility of the fluid-saturated rock

The undrained compressibility C_{ud} (or bulk modulus $K_{ud} = C_{ud}^{-1}$) (Table 1) of a rock subjected to isotropic compression and strain refers to its poroelasticity before any fluid leaves the pore space and after any pore-scale inhomogeneities of fluid pressure have relaxed. That is, pressures are equilibrated throughout the pore space (Biot, 1941; Gassmann, 1951; Jaeger et al., 2007; Mavko et al., 2009; Thomsen, 2020). Seismic and, in most cases, sonic P-wave velocities of conventional reservoir rocks can be computed from $V_P = (M_{ud}/\rho_b)^{0.5}$, where ρ_b is the bulk density, and $M_{ud} = K_{ud} + (4/3)G$ is the P-wave modulus of the undrained rock and G is its shear modulus that is independent of the fluid saturation in the case of nonviscous fluids. Because the bulk density dependence on fluid saturation is straightforward (a volumetric weighted average of the rock components), our ability to predict fluid saturation from seismic or sonic data hinges solely on our understanding of its effects on the undrained bulk modulus.

The decision to write this paper was motivated by recent publications by Thomsen (2020, 2021), who demonstrated that under certain circumstances (e.g., rock microstructure or fluid compressibility) Gassmann's equation for K_{ud} may overestimate the effect of fluid saturation. A well-known form of this equation is

$$K_{ud} = K_d + \beta^2 \left[\frac{\phi}{K_f} + \frac{\beta - \phi}{K_m} \right]^{-1}, \quad (1)$$

where K_d is the dry rock bulk modulus, K_f and K_m are the bulk moduli of the effective fluid and mineral phases, respectively, ϕ is the total porosity, and β is the Biot coefficient (Table 1) defined as $\beta = 1 - K_d/K_m$. The undrained compressibility form of Gassmann's equation is

$$C_{ud} = C_d - \frac{(C_d - C_m)^2}{\phi(C_f - C_m) + C_d - C_m}. \quad (2)$$

The four main assumptions that are made when applying Gassmann's equation are: (1) pore pressure is equilibrated throughout the pore space, (2) all the constituent minerals are linearly elastic and have the same bulk and shear moduli, (3) the rock is isotropic, and (4) the rock is fully saturated with low-viscosity fluids. Although challenged by several experimental results on sedimentary rocks, Gassmann's equation is usually assumed to be independent of the pore-space microstructure and applicable to any *compositionally* microhomogeneous rock (Mavko et al., 2009). This concept was questioned in recent papers by Thomsen (2020, 2021), who suggested that more accurate but also more complex models, such as those by Biot (1941) and Brown and Korringa (1975), must be used. Although still dependent on the aforementioned list of assumptions, both models consider four independent moduli (or compressibilities) instead of only the three (K_d, K_f, and K_m) used in Gassmann's equation to take into account the effect of the pore-space microstructure on the undrained rock compressibility. For example, Brown and Korringa (1975) introduced a new mean compressibility C_M (Table 1) that corresponds to the unjacketed bulk compressibility of the rock and relates to Biot's poroelastic parameters H and R as follows: $H^{-1} = C_d - C_M$ and $R^{-1} = H^{-1} - \phi C_M$. Brown-Korringa's equation in its general form is given by Thomsen (2020) as

$$C_{ud} = C_d - \frac{(C_d - C_M)^2}{\phi(C_f - C_m') + C_d + C_m' - 2C_M}, \quad (3)$$

where C_m' is the unjacketed solid material compressibility. It is related to the unjacketed bulk compressibility $C_M = (1 - \phi) C_m' + \phi C_\phi$, where C_ϕ is the unjacketed pore volume compressibility. Brown

and Korringa (1975) argue that their model is reduced to Gassmann's equation in the case of a compositionally micro-homogeneous rock, which is assumed synonymous to a monomineralic rock, or a rock comprised of minerals with similar elastic properties. Indeed, if $C_M = C'_m = C_m$ (which also implies that $C_\phi = C_m$), equation 3 is reduced to equation 2. However, in the case of microheterogeneous rocks, C'_m differs from the effective mineral compressibility C_m, and the difference between the undrained rock compressibilities predicted by equations 2 and 3 increases with the difference between C'_m (or C_M) and C_m. Although using Brown-Korringa's equation would be preferable, experimentally measuring unjacketed compressibilities remains a technical challenge, especially for C_ϕ, which relies on precise measurements of pore volume variations as a function of pore pressure. For that reason, Brown-Korringa's equation remains rarely applied in practice.

However, Thomsen (2020) suggests that the microhomogeneity restriction is not responsible for the difference between C_M and C_m, attributing it rather to "a logical error made by both Gassmann and Brown and Korringa." The error lies in the application of the unjacketed (hydraulically open) condition, where differential pressure (confining pressure minus pore fluid pressure) is kept constant so the solid material compressibility remains the only parameter governing the variations in rock volume. Therefore, according to Thomsen (2020), equation 3 applies to all macro-isotropic uniform rocks with equilibrated pore pressure. Furthermore, Thomsen (2020) suggests that Biot's poroelastic modulus H (and therefore C_M) can be determined from the ratio of undrained fluid pressure to confining pressure (i.e., Skempton's coefficient $B = P_p/\sigma$ [Table 1]) in a quasi-static laboratory experiment:

$$B = \frac{C_d - C_{ud}}{C_d - C_M} = H(C_d - C_{ud}). \qquad (4)$$

Unfortunately, this type of experiment remains too rare, expensive, and inconclusive to enable a routine application of Brown-Korringa's equation. Importantly, Thomsen (2021) also hints that C_M may depend on the effective stress and microgeometry of the rock but does not specify how. This leads us to consider this parameter and its impact on fluid substitution modeling in the framework of the Vernik-Kachanov rock physics model.

Vernik-Kachanov model: Revisited

Vernik and Kachanov (2010) introduced a rock physics model (V-K model) for isotropic rocks, which is based on the separation and different parameterization of the compliance contributions of pores and cracks (and/or grain contact and intragrain microcracks). Cracks are approximated as spheroids of very low and variable aspect ratio $\alpha < 0.01$, although typical cracks fall below

Table 1. Definitions of various poroelastic compressibilities and coefficients. A porous sample is comprised of a solid material phase occupying an initial volume V_m^i and a fluid phase residing in the initial pore volume V_p^i so that the initial bulk volume of the sample is $V_b^i = V_m^i + V_p^i$. The constants are defined in terms of confining (P_c), fluid (P_f), and differential ($P_d = P_c - P_f$) pressures. Drained or dry conditions mean that the fluid mass is null ($m_f = 0$). Undrained or saturated conditions mean that the fluid mass remains constant. Unjacketed conditions means that the differential pressure remains constant. ε_m is the volumetric strain of the solid material.

Poroelastic constant	Symbol	Definition
Effective mineral compressibility	$C_m = \dfrac{1}{K_m}$	$-\dfrac{1}{V_m^i}\dfrac{dV_m}{dP_c}$
Effective fluid compressibility	$C_f = \dfrac{1}{K_f}$	$-\dfrac{1}{V_p^i}\dfrac{dV_p}{dP_c}$
Drained or dry rock bulk compressibility	$C_d = \dfrac{1}{K_d}$	$-\dfrac{1}{V_b^i}\left(\dfrac{\partial V_b}{\partial P_c}\right)_{m_f=0}$
Drained or dry rock pore space compressibility	$C_p = \dfrac{1}{K_p}$	$-\dfrac{1}{V_p^i}\left(\dfrac{\partial V_p}{\partial P_c}\right)_{m_f=0}$
Undrained or saturated rock bulk compressibility	$C_{ud} = \dfrac{1}{K_{ud}}$	$-\dfrac{1}{V_b^i}\left(\dfrac{\partial V_b}{\partial P_c}\right)_{m_f}$
Unjacketed bulk compressibility	$C_M = \dfrac{1}{K_M}$	$-\dfrac{1}{V_b^i}\left(\dfrac{\partial V_b}{\partial P_f}\right)_{P_d}$
Unjacketed solid material compressibility	$C'_m = \dfrac{1}{K'_m}$	$-\dfrac{1}{V_m^i}\left(\dfrac{\partial V_m}{\partial P_f}\right)_{P_d}$
Unjacketed pore space compressibility	$C_\phi = \dfrac{1}{K_\phi}$	$-\dfrac{1}{V_p^i}\left(\dfrac{\partial V_p}{\partial P_f}\right)_{P_d}$
Bulk volume effective pressure coefficient	ψ	$\left(\dfrac{\partial P_c}{\partial P_f}\right)_{\varepsilon_m=0}$
Biot coefficient	β	$-\left(\dfrac{\partial V_p}{\partial V_b}\right)_{m_f=0}$
Skempton coefficient	B	$\left(\dfrac{\partial P_f}{\partial P_c}\right)_{m_f}$

0.005 (e.g., Jaeger et al., 2007). Pores can have a variety of 3D geometries that typically do not resemble, even remotely, spheroids or ellipsoids. By and large, pores contribute to the total porosity, whereas cracks and microcracks control the stress sensitivity of elastic velocities and permeability in most reservoir rocks. The V-K model for consolidated sediments (e.g., sandstones and limestones) is based on the Mori-Tanaka effective field theory and yields the dry rock moduli as (Vernik and Kachanov, 2010; Vernik, 2016)

$$K_d = K_m \left[1 + \frac{p\phi}{1-\phi} + A(v_m)\eta_0 \frac{\exp(-d\sigma)}{1-\phi} \right]^{-1} \qquad (5a)$$

$$G_d = G_m \left[1 + \frac{q\phi}{1-\phi} + B(v_m)\eta_0 \frac{\exp(-d\sigma)}{1-\phi} \right]^{-1}, \qquad (5b)$$

where $A(v_m)$ and $B(v_m)$ are known functions of the Poisson's ratio of the solid material (e.g., Benveniste, 1987), $\eta_0 = na^3/V$ is the initial or zero-stress crack density parameter (Bristow, 1960) (n/V is the number of cracks per unit volume and a is the mean crack length), σ is the effective stress, and d is the crack aspect ratio distribution-dependent coefficient, which (based on laboratory measurement of velocity versus stress on dry sandstones and carbonates) generally varies between 0.05 and 0.07. The model given by equations 5a and 5b is strictly valid for rocks with porosity lower than the consolidation porosity (ϕ_{con} that usually ranges between 22% and 32%). At that point, it can be extended by an empirical leg connecting the moduli at the consolidation porosity with the moduli at the critical porosity close to the earth's surface onshore or the mudline offshore. The entire model is designed to describe the effect of compaction and diagenesis (first mechanical, then chemical) on dry elastic moduli.

The second part in the brackets of equations 5a and 5b represents the compliance contribution due to pores, while the effect of elastic interactions is accounted for by the Mori-Tanaka multiplier $(1 - \phi)^{-1}$ applied to both the second and third parts. According to Jaeger et al. (2007), some of the simpler pore shapes, such as tetrahedrons, cubes, rectangles, and hypotrochoids (with cusped corners), lend themselves for 2D mapping in terms of their geometry factors relative to those of a sphere. Pore-space compressibilities in isotropic and shear conditions can be expressed as a product of matrix compressibility and volumetric and deviatoric strain concentration factors p and q, respectively (Kachanov et al., 1994). These quantities, usually referred to as pore-shape factors, are explicit functions of the Poisson's ratio of the solid material for spheroidal pores (e.g., Berryman, 1980b). The numerical values of p and q can be relatively well constrained, even for more complex shapes in 2D, given the petrographic observations of the pore perimeters and areas (Jaeger et al., 2007; Mur and Vernik, 2020). In-situ log data acquired in carbonates and arenite sandstones (with 2% to 12% of structural and matrix clay) with $\phi < \phi_{con}$ can be accurately described using equations 5a and 5b with the

following empirical pore-shape factor expressions: $p = (p_{sphere} + t) + b_p\phi$ and $q = (q_{sphere} + t) + b_q\phi$, where p_{sphere} and q_{sphere} are the pore-shape factors of spherical pores, $t = 1.2$ to reflect the fact that at very low porosity the pore geometry is generally not spherical but closer to tetragonal, and b_p and b_q generally range between 10 and 20 (Vernik and Gallop, 2022).

The third part in the brackets of equations 5a and 5b corresponds to the compliance contribution of cracks. The crack density parameter $\eta = \eta_0 \exp(-d\sigma)$ can vary from 0 with no stress sensitivity to as high as 2 or 3 (strongly dependent on the crack length), where percolation can be achieved and ultimately lead to disintegration. However, even rocks with intermediate η values between 0.1 and 0.3 may exhibit significant stress sensitivity of their P- and S-wave velocities. A convenient feature of equations 5a and 5b, inherited from the Mori-Tanaka effective field theory, is decoupling between the crack density term and the term containing porosity and pore-shape factors. Because the aspect ratio (α) of spheroids barely affects their compliance when their diameters are kept constant and α is reduced below 0.1 (Sevostianov and Kachanov, 2011), it indeed makes sense to use the crack density rather than the crack porosity as a parameter in elasticity formulations for cracks with $\alpha < 0.01$. Practically, the zero-stress crack density η_0 can be constrained as a linear function of porosity in sandstones and carbonates using $\eta_0 = c_1 + c_2\phi$, with c_1 ranging between 0.02 and 0.25 and c_2 usually about 2 (Vernik, 2016).

Vernik (2016) uses equations 5a and 5b in combination with Gassmann's equation to predict the effects of fluid saturation on seismic and, in most cases, even sonic wave velocities in reservoir
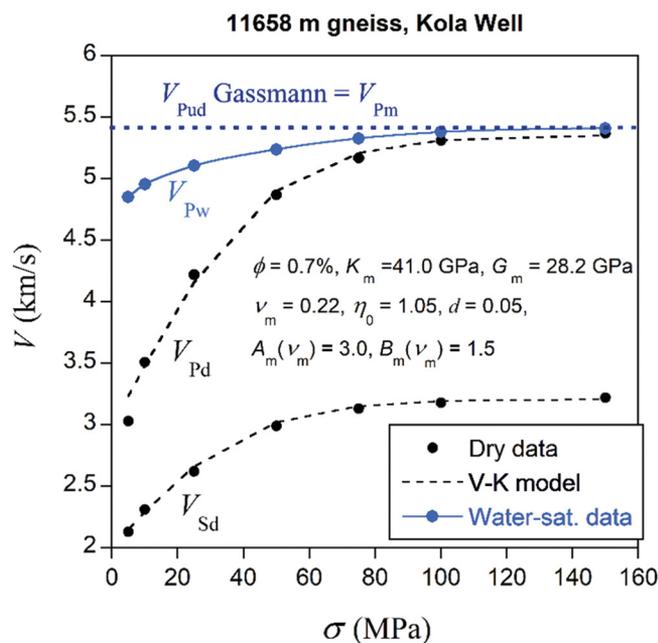
Figure 1. Dry- and water-saturated ultrasonic P-wave velocities versus confining stress in the gneiss core from a depth of 11,700 m in the Kola well (Vernik et al., 1994) superimposed on the Vernik-Kachanov rock physics model calibrated with the indicated parameters. Note how Gassmann's-equation-based undrained V_{Pud} remains equal to the solid material velocity V_{Pm} and is larger than the measured (unrelaxed) water-saturated velocity V_{Pw}, regardless of the stress applied to this rock with extremely low porosity and high microcrack density induced by core recovery.

rocks. The workflow was noted to produce dramatic change in slope in the velocity versus porosity space at porosity below 1%–2%, where the crack density effect dominates elastic moduli. On the other hand, Gassmann's theory remains questionable when applied to very low-porosity rocks with significant microstructural inhomogeneity (Müller and Sahay, 2014). To further investigate the issue, we resort to analysis of the data generated by Vernik et al. (1994) on an Archean gneiss core recovered from the Kola well at a depth of 11,700 m (38,300 ft). Both stress release (from more than 300 MPa in situ) and cooling (from more than 200°C in situ) resulted in the formation of microcracks, which impart dramatic stress sensitivity to this

Figure 2. (a) V-K-model-based dry bulk modulus versus porosity for a sandstone characterized by a relatively low effective stress of 19 MPa (in the consolidated regime) and significant crack density. This is compared to Gassmann-based predictions (thin lines) for brine- (K_{br} = 3.6 GPa) and light-oil- (K_o = 0.9 GPa) saturated cases and the generalized B-K model of equation 6, with K_M and K'_m moduli computed using equations 7a and 7b (thick lines). (b) Undrained P-wave velocity versus porosity using the same rock physics model combined with Gassmann predictions for gas (K_g = 0.25 GPa), oil, and brine (thin lines) compared to those of equations 6, 7a, and 7b (thick lines).

rock sample comprised of quartz, plagioclase, and about 22% micas. The benchtop porosity of this gneiss is about 1% (totally attributable to microcracks), which makes it a convenient example to illustrate the impact of compliant cracks on dry and saturated rock compressibilities in the absence of stiffer pores. As shown in Figure 1, the stress dependence of dry ultrasonic velocities in this crystalline rock with extremely low porosity is successfully modeled using equations 5a and 5b, where the solid material moduli were tentatively derived from the measurements at 150 MPa (i.e., at a confining stress approaching the crack closure stress of this damaged rock sample). Not surprisingly, given such large stress release and cooling effects, the zero-stress crack density of η_0 = 1.05 inverted from the model calibration turns out to be extremely high. Application of Gassmann's equation to the entire spectrum of stress-dependent data on this rock with extremely low porosity yields $K_{ud} \approx K_m$ and a P-wave velocity of $V_{Pud} \approx V_{P@150MPa}$. The latter result is included in Figure 1 as the dashed horizontal line to be compared with the fully water-saturated ultrasonic V_{Pw} in the same experiment. This represents the *undrained* and *unrelaxed* (in terms of pore-pressure equilibration) response, which, by definition, must satisfy inequality $V_{Pw} > V_{Pud}$. This example clearly shows that Gassmann's equation can lead to large prediction errors when applied to cracked rocks with extremely low porosity and, more generally, any rock that does not satisfy $K_{ud}|_{\phi=0} = K_d|_{\phi=0} = K_m$.

While practical implications for such low-porosity rocks may not be of concern, the same inaccuracy persists for higher-porosity consolidated reservoir rocks if the void space presents a combination of pores and cracks, which is almost always the case in sandstones and carbonates, notably at low effective stress. Because Gassmann's equation may exaggerate the fluid incompressibility effect, and the magnitude of the error depends on the difference between C_M and C_m (Thomsen, 2020), we suggest using Brown-Korringa's equation instead of Gassmann's equation for any rock containing even a minor number of cracks and subject to an effective stress that is significantly lower than the crack closure stress ($\sigma_{closure}$). In the same manner that equation 3 can be compared

with equation 2, the following reformulation of Brown-Korringa's equation in terms of moduli is proposed for a direct comparison with equation 1:

$$K_{ud} = K_d + \psi^2 \left[\frac{\phi}{K_f} + \frac{1-\phi}{K'_m} + \frac{\psi-1}{K_M} \right]^{-1}, \quad (6)$$

where ψ is the bulk volume effective pressure coefficient (Table 1) of a microheterogeneous rock defined as $\psi = 1 - K_d/K_M$ (Müller and Sahay, 2016). To apply equation 6 in practice, we also suggest the following expressions derived from the V-K model for the unjacketed bulk modulus and unjacketed solid material bulk modulus of a microheterogeneous rock with cracks:

$$K_M = K_m \left[1 + A(v_m)\eta_0 \exp(-d\sigma) \right]^{-1} \quad (7a)$$

$$K'_m = \lim_{\phi \to 0}(K_M) = K_m \left[1 + A(v_m)c_1 \exp(-d\sigma) \right]^{-1}, \quad (7b)$$

where c_1 is the intercept of the linear function of porosity used to model η_0. The second part in the brackets of equation 7a is the compliance contribution to the dry frame compressibility due to cracks from equation 5a. It is important to note that K'_m, defined as the limit of K_M when porosity tends to 0, is not a directly measurable property for rock samples with cracks subjected to an effective stress that is lower than the crack closure stress. It only becomes measurable at an effective stress that is higher than crack closure stress or for samples without cracks, in which case it reduces to K_m. In agreement with Thomsen (2020), the introduction of equations 7a and 7b to compute K_M and K'_m has nothing to do with micro-inhomogeneity in terms of the variations in mineral moduli of the solid material, but it is totally driven by the crack density term in the V-K model. Note that in poorly consolidated sediments (i.e., those with porosity greater than ϕ_{con}), the effect described by equations 6, 7a, and 7b is implicitly contained in the

dry rock moduli at the consolidation porosity and gradually decreases as porosity increases beyond that threshold value. The discrepancy between Gassmann's and Brown-Korringa's predictions is illustrated in Figures 2a and 2b, which plot bulk modulus and P-wave velocity as a function of porosity and show that Gassmann's modeling inaccuracy, which increases with crack density, is also proportional to the fluid incompressibility (i.e., the error is greater in brine-saturated rocks than in hydrocarbon-saturated ones). Note that the unstable behavior of the model lines at a porosity of less than 2% is no longer observed with the proposed alternative model.

For the case considered in Figures 2a and 2b, Gassmann's velocity overprediction in brine-saturated sandstone with relatively high crack density ($\eta > 0.2$) reaches a relative maximum of 3% in the 15%–25% porosity range. It is tapered to 2% as porosity is reduced from this level to 5% or increased to 35%. The oil case in Figures 2a and 2b is based on a light oil with a high gas/oil ratio. The oil versus gas case velocity difference decreases from a relative average of 1.6% for Gassmann's model to a mere 0.3% when using Brown-Korringa's equation.

The model comparison is further exemplified in Figure 3, which shows a log plot of a deep 23±1% porosity sandstone reservoir with an oil saturation of about 75%, transitioning to a water leg downhole. The reservoir is significantly overpressured, resulting in a low vertical effective stress of 19 MPa. The low-frequency velocity from the Gassmann's equation-based oil-to-brine substitution is shown to be about 3% greater than the low-frequency velocity predicted using the combination of equations 6, 7a, and 7b. The unjacketed bulk modulus K_M in these equations is a function of the effective mineral bulk modulus K_m and the stress-dependent crack density parameter η, with zero-stress crack density $\eta_0 = 0.2 + 2\phi$ in this example. Due to the sensitivity of K_m to the clay volume fraction, it is challenging to compare the modeled brine-saturated P-wave velocity log in the reservoir to the actual sonic velocity below the oil-water contact. However, for a similar sandstone composition, the velocity predicted from equations 6, 7a, and 7b appears qualitatively more consistent than the higher velocity predicted with Gassmann's model. Further investigations under different stress conditions may shed light on the practical significance of replacing Gassmann's model with the model suggested in this work.

However, at this point we can state that Gassmann's result is only accurate in rocks with extremely low crack density, (i.e., with very low zero-stress crack density or subject to very high effective stress approaching crack closure stress, where even the most inflated cracks start to close, so that crack density exponentially tends to zero). This suggests that the difference $(K_m - K_M)$ and the error in Gassmann's prediction of the fluid incompressibility effect on seismic velocity may simply be related to $\eta_0[1 - \exp(-d\sigma)]$. Published laboratory measurements of velocities versus stress obtained on dry reservoir rocks, instead of new (challenging, expensive, and often inconclusive [Duranti, 2018]) quasi-static experiments to determine Skempton's pore-pressure buildup coefficient (B) on fluid-saturated rocks, may be sufficient to constrain Gassmann's error. In fact, the evasive η_0 term can be accurately quantified through parameter optimization when calibrating the proposed model (specifically, equations 5a and 5b) to dry rock laboratory data.
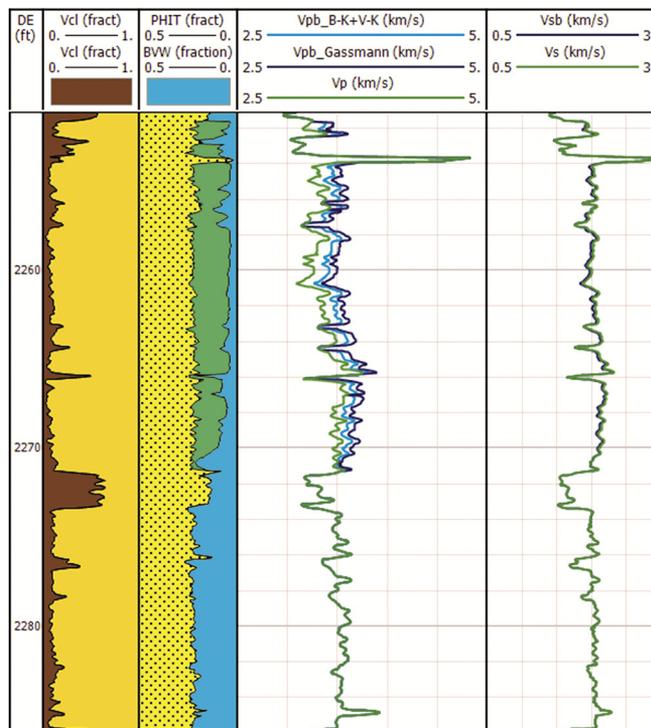
Figure 3. Example of a 23±1% porosity overpressured oil sandstone reservoir transitioning to a water leg below 2270 ft. Measured sonic P- and S-wave velocities are shown in green. The blue curves represent the fully brine-saturated reservoir interval using Gassmann's equation (dark blue) and equations 6, 7a, and 7b (light blue), showing a difference of up to 0.1 km/s or 3%.

Quantification of compliance to Gassmann's assumptions

Although the applicability of Gassmann's theory to a particular rock is a recurrent topic of discussion, few authors have attempted to quantify the deviation of rock behavior to the requirements of Gassmann's model. Among these authors, Sahay (2013) defines a micro-inhomogeneity parameter n (referred to simply as a homogeneity parameter hereafter) with a value of 1 for Gassmann-compliant rocks and values that deviate from 1 for rocks that violate Gassmann's assumptions. According to Müller and Sahay (2014), the potential deformational energy due to a stress applied to a rock "can become partially localized in the interfacial region due to surface roughness or within the bulk part of the solid due to a multimineral frame." Both features constitute violations of Gassmann's assumptions. We further suggest that cracks present in a rock act as focal points for partial localization of deformational energy and contribute to the softening effect as compared to the behavior postulated in Gassmann's theory. Some of this softening may be explained in part by fluid flowing out of the compliant cracks into stiffer pores, a phenomenon often referred to as local or squirt flow effect. In their generalized poroelasticity framework for micro-inhomogeneous rocks, Müller and Sahay (2016) highlight the need to express the homogeneity parameter in terms of measurable quantities to be of any use in practice. Based on equations 5a, 5b, 7a, and 7b, the homogeneity parameter can be conveniently reformulated as a function of measurable effective stress and quantifiable crack density and volumetric pore-shape factor:
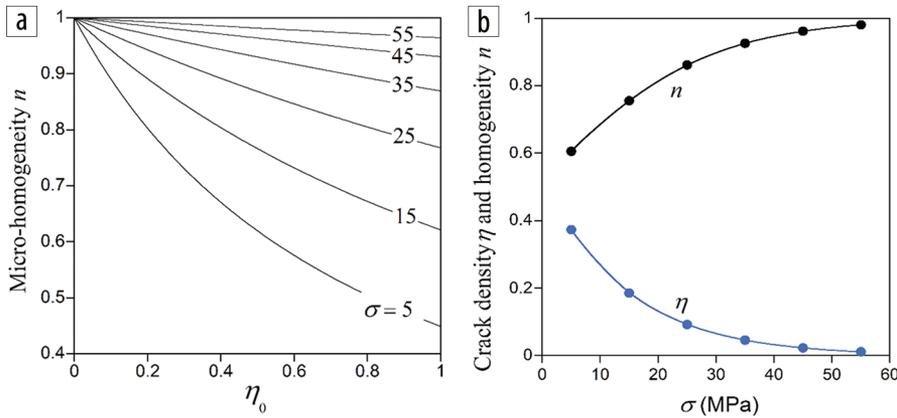
Figure 4. (a) Homogeneity parameter as a function of zero-stress crack density and effective stress (in MPa) in arenite-type 23% porosity sandstone with a pore-shape factor p of 7.1. (b) Evolution of effective crack density and homogeneity parameters as a function of effective stress applied to the same rock as in (a), illustrating how deviation from Gassmann's compliance ($n = 1$ or $\eta = 0$) decreases with increasing effective stress.

$$n = \frac{\psi - \phi}{\beta' - \phi} = \left[1 + \frac{A(v_m)c_2\exp(-d\sigma)}{p - 1}\right]^{-1}, \qquad (8)$$

where c_2 is the slope of the linear function of porosity used to model η_0. By definition, n varies according to the difference between the bulk volume effective pressure coefficient of a microheterogeneous rock ($\psi = 1 - K_d/K_M$) and the Biot coefficient of a microheterogeneous rock ($\beta' = 1 - K_d/K_m'$). In the case of microhomogeneous rocks with no cracks or microheterogeneous rocks with cracks subjected to pressures higher than the closure pressure, both coefficients reduce to the familiar form $1 - K_d/K_m$ and therefore $n = 1$. In contrast, for microheterogeneous rocks with cracks subjected to pressures lower than the closure pressure, $K_M < K_m'$, leading to $n < 1$. This effect is illustrated in Figure 4a, which shows how larger zero-stress crack density and lower effective stress reduce n in a 23% porosity sandstone with an average pore-shape factor p of 7.1. Figure 4b highlights how, for the same sandstone with relatively high zero-stress crack density η_0 of 0.66, an increase in effective stress from 5 to 55 MPa reduces its effective crack density and increases its homogeneity parameter, resulting in a state ever closer to Gassmann's compliance. Note that the proposed model only accounts for the elastic crack closure. If the increase in effective or deviatoric stress causes inelastic deformation, such as grain sliding and crushing, the homogeneity parameter can start diverging away from Gassmann's compliance, as observed in published laboratory data (Figure 1 in Müller and Sahay [2016]).

Thomsen (2020) and Müller and Sahay (2014) suggest that the assessment of Gassmann's applicability is primarily dependent on the ability to determine Skempton's B coefficient based on laboratory quasi-static deformation experiments, which present many challenges of their own and are not common. Based on equation 8, we suggest again that much more routine, straightforward, and less controversial laboratory measurements of velocities versus stress obtained on dry reservoir rocks are sufficient to calibrate the crack density parameter, derive (optionally) the homogeneity parameter, and apply the more general Brown-Korringa's equation (instead of Gassmann's equation) to perform accurate forward modeling for a wide range of reservoir rocks under any stress state.

Conclusions

The application of Gassmann's equation to estimate fluid effects on P-wave velocity in reservoir rocks can be substantially inaccurate for porous rocks with moderate to high crack density. This is typically the case when the zero-stress crack density parameter is high or effective stress is low. Although not the sole cause of inaccuracy, Gassmann's prediction error is directly affected by the stress sensitivity induced by the presence of microcracks in the reservoir rock. Because the stress sensitivity can be evaluated using the crack density parameter and its exponential decay with effective stress due to crack closure, it is not necessary to conduct expensive laboratory experiments to obtain Skempton's coefficient. Instead, we suggest that calibrating the Vernik-Kachanov rock physics model to match existing laboratory-measured stress-dependent dry rock velocities may be sufficient to quantify Gassmann's applicability and use the more general Brown-Korringa's fluid substitution equation. Finally, evaluating the magnitude of inaccuracies due to the use of simple Gassmann-based fluid substitution modeling can be especially challenging in forward modeling of seismic and sonic velocities when limited information on interval velocity is available to control the quality of the modeled P-wave velocity. **TLE**

Data and materials availability

Data associated with this research are confidential and cannot be released.

Corresponding author: fabien.allo@cgg.com

References

Benveniste, Y., 1987, A new approach to the application of Mori-Tanaka's theory in composite materials: Mechanics of Materials, **6**, no. 2, 147–157, https://doi.org/10.1016/0167-6636(87)90005-6.

Berryman, J. G., 1980a, Long-wavelength propagation in composite elastic media I: Spherical inclusions: Journal of the Acoustical Society of America, **68**, 1809–1819, https://doi.org/10.1121/1.385171.

Berryman, J. G., 1980b, Long-wavelength propagation in composite elastic media II: Ellipsoidal inclusions: Journal of the Acoustical Society of America, **68**, 1820–1831, https://doi.org/10.1121/1.385172.

Biot, M. A., 1941, General theory of three-dimensional consolidation: Journal of Applied Physics, **12**, no. 2, 155–164, http://doi.org/10.1063/1.1712886.

Bristow, J. R., 1960, Microcracks and the static and dynamic elastic constants of annealed heavily cold-worked metals: British Journal of Applied Physics, **11**, no. 2, 81–85, https://doi.org/10.1088/0508-3443/11/2/309.

Brown, R. J. S., and J. Korringa, 1975, On the dependence of the elastic properties of a porous rock on the compressibility of the pore fluid: Geophysics, **40**, no. 4, 608–616, https://doi.org/10.1190/1.1440551.

Duranti, L., 2018, On the homogeneity of poroelastic media: Experimental measurements of Kϕ: 88th Annual International Meeting, SEG, Expanded Abstracts, 3537–3541 https://doi.org/10.1190/segam2018-2998972.1.

Gassmann, F., 1951, Über die Elastizität poröser Medien: Vierteljahrsschrift der Naturforschenden Gesellschaft in Zürich, **96**, 1-23.

Jaeger, J. C., N. G. W. Cook, and R. W. Zimmerman, 2007, Fundamentals of rock mechanics, fourth edition: Wiley-Blackwell.

Kachanov, M., I. Tsukrov, and B. Shafiro, 1994, Effective moduli of solids with cavities of various shapes: Applied Mechanics Reviews, **47**, no. 1S, S151–S174, https://doi.org/10.1115/1.3122810.

Mavko, G., T. Mukerji, and J. Dvorkin, 2009, The rock physics handbook: Tools for seismic analysis of porous media, second edition: Cambridge University Press, https://doi.org/10.1017/CBO9780511626753.

Müller, T. M., and P. N. Sahay, 2014, Skempton coefficient and its relation to the Biot bulk coefficient and micro-inhomogeneity parameter: 84th Annual International Meeting, SEG, Expanded Abstracts, 2905–2909 https://doi.org/10.1190/segam2014-0446.1.

Müller, T. M., and P. N. Sahay, 2016, Generalized poroelasticity framework for micro-inhomogeneous rocks: Geophysical Prospecting, **64**, no. 4, 1122–1134, https://doi.org/10.1111/1365-2478.12392.

Mur, A., and L. Vernik, 2020, Rock physics modeling of carbonates: 90th Annual International Meeting, SEG, Expanded Abstracts, 2479–2483, https://doi.org/10.1190/segam2020-3427703.1.

Sahay, P. N., 2013, Biot constitutive relation and porosity perturbation equation: Geophysics, **78**, no. 5, L57–L67, https://doi.org/10.1190/geo2012-0239.1.

Sevostianov, I., and M. Kachanov, 2011, Elastic fields generated by inhomogeneities: Far-field asymptotics, its shape dependence and relation to the effective elastic properties: International Journal of Solids and Structures, **48**, no. 16–17, 2340–2348, https://doi.org/10.1016/j.ijsolstr.2011.04.014.

Thomsen, L., 2020, A logical error in Gassmann poroelasticity: 90th Annual International Meeting, SEG, Expanded Abstracts, 2429–2433, https://doi.org/10.1190/segam2020-3424536.1.

Thomsen, L., 2021, The logical error in Gassmann poroelasticity: Consistency with effective medium theory: 1st International Meeting for Applied Geoscience & Energy, SEG/AAPG, Expanded Abstracts, 2303–2307, https://doi.org/10.1190/segam2021-3580471.1.

Vernik, L., 2016, Seismic petrophysics in quantitative interpretation: SEG, https://doi.org/10.1190/1.9781560803256.

Vernik, L., and M. Kachanov, 2010, Modeling elastic properties of siliciclastic rocks: Geophysics, **75**, no. 6, E171–E182, https://doi.org/10.1190/1.3494031.

Vernik, L., and J. Gallop, 2022, Elastic depth trends for siliciclastic sequences: Geophysics, **87**, no. 1, MR25–MR34, https://doi.org/10.1190/segam2020-3428179.1.

Vernik, L., S. Hickman, D. Lockner, and M. Rusanov, 1994, Ultrasonic velocities in cores from the Kola superdeep well and the nature of subhorizontal seismic reflections: Journal of Geophysical Research: Solid Earth, **99**, no. B12, 24209–24219, https://doi.org/10.1029/94JB01236.